

# Rapid Rotation, Active Nests of Convection and Global-scale Flows in Solar-like Stars

B.P. Brown<sup>1,\*</sup>, M.K. Browning<sup>2</sup>, A.S. Brun<sup>1,3</sup>, M.S. Miesch<sup>4</sup>, and J. Toomre<sup>1</sup>

<sup>1</sup> JILA and Dept. of Astrophysical & Planetary Sciences, University of Colorado, Boulder, CO 80309-0440

<sup>2</sup> Dept. of Astronomy, University of California, Berkeley, CA 94720-3411

<sup>3</sup> DSM/DAPNIA/SAP, CEA Saclay, Gif sur Yvette, 91191 Cedex, France

<sup>4</sup> High Altitude Observatory, NCAR, Boulder, CO 80307-3000

The dates of receipt and acceptance should be inserted later

**Key words** stars: interiors – stars: rotation – Sun: interior – hydrodynamics – methods: numerical

In the solar convection zone, rotation couples with intensely turbulent convection to build global-scale flows of differential rotation and meridional circulation. Our sun must have rotated more rapidly in its past, as is suggested by observations of many rapidly rotating young solar-type stars. Here we explore the effects of more rapid rotation on the patterns of convection in such stars and the global-scale flows which are self-consistently established. The convection in these systems is richly time dependent and in our most rapidly rotating suns a striking pattern of spatially localized convection emerges. Convection near the equator in these systems is dominated by one or two patches of locally enhanced convection, with nearly quiescent streaming flow in between at the highest rotation rates. These active nests of convection maintain a strong differential rotation despite their small size. The structure of differential rotation is similar in all of our more rapidly rotating suns, with fast equators and slower poles. We find that the total shear in differential rotation, as measured by latitudinal angular velocity contrast,  $\Delta\Omega$ , increases with more rapid rotation while the relative shear,  $\Delta\Omega/\Omega$ , decreases. In contrast, at more rapid rotation the meridional circulations decrease in both energy and peak velocities and break into multiple cells of circulation in both radius and latitude.

© 2007 WILEY-VCH Verlag GmbH & Co. KGaA, Weinheim

## 1 Rotation and Dynamo Action

Rotation and magnetism couple with turbulent plasma motions in stellar convection zones to drive dynamos and cycles of magnetic activity. When our sun was younger, it must have rotated more rapidly, as is suggested by observations of rapidly rotating young solar-like stars and by the presence of the magnetized solar wind, which continually removes angular momentum from the star. Observations of rapidly rotating stars indicate that generally more rapid rotation is correlated with stronger magnetism and perhaps stronger dynamo action. In the sun, global-scale dynamo action is thought to arise from the coupling of convection and rotation. Here we explore the effects of more rapid rotation on global-scale convective structures and in particular on the resulting differential rotation and meridional circulation.

Helioseismology, which uses acoustic oscillations at the solar surface to probe the radial and latitudinal structure of the star as well as the convective flows beneath the surface, has revealed that the solar differential rotation profile observed at the surface prints throughout the convection zone with two prominent regions of radial shear. The near-surface shear layer exists in the outer 5% of the sun, and the tachocline lies between the differentially-rotating convection zone and the deeper radiative interior, which is

in nearly solid body rotation (Thompson et al. 2003). These shear layers, combined with the global-scale flows of meridional circulation and differential rotation, are thought to be the key components in the global solar dynamo which builds and rebuilds magnetic fields yielding 22-year cycles of magnetic activity. In the interface dynamo model (e.g., Charbonneau 2005; Ossendrijver 2003), magnetic fields generated in the bulk of the convection zone are pumped downward into the tachocline where the strong radial shear builds large-scale fields that eventually erupt at the solar surface. The differential rotation plays an important role both in building and organizing the global-scale fields while the meridional circulations may be important for returning flux to the base of the convection zone, enabling cycles of magnetic activity. The nature of internal differential rotation in other stars is unclear, though some observations of the surface differential rotation are now possible through a variety of techniques including photometric variability (Donahue et al. 1996; Walker et al. 2007), Doppler imaging (Donati et al. 2003) and Fourier transform methods (Reiners & Schmitt 2003). We undertake simulations to self-consistently establish differential rotation through the coupling of convection and rotation to study this crucial ingredient for stellar dynamo action.

\* Corresponding author: e-mail: bpbrown@solarz.colorado.edu

## 2 Simulations of rapidly rotating suns

To capture the essential couplings between convection, rotation and the resulting global-scale flows, we must employ a global model which simultaneously includes the spherical shell geometry and admits the possibility of zonal jets, large eddy vortices and convective plumes which may span the depth of the convection zone. The solar convection zone is intensely turbulent and molecular values of viscosity and thermal diffusivity in the sun are estimated to be very small. As a consequence, numerical simulations cannot hope to resolve all scales of motion present in real solar convection and a compromise must be struck between faithfully capturing the important dynamics within small regions and capturing the connectivity and geometry of the global scales.

### 2.1 The ASH code

Our tool for exploring stellar convection is the anelastic spherical harmonic (ASH) code, which is described in detail in Clune et al. (1999) and in Brun et al. (2004). ASH is a mature simulation code, designed to run on massively parallel architectures, which solves the three-dimensional MHD equations of motion under the anelastic approximation. The velocity field is fully nonlinear, but under the anelastic approximation the thermodynamic variables are linearized about their spherically symmetric and evolving mean state with density  $\bar{\rho}$ , pressure  $\bar{P}$ , temperature  $\bar{T}$  and specific entropy  $\bar{S}$  all varying with radius. The overall density contrast is about 25 between the top and bottom of the simulation.

As a global-scale code, ASH cannot resolve all scales of motion present in real stellar convection zones. Instead, we conduct large eddy simulations (LES) which explicitly resolve the largest scales and describe scales below the grid resolution with subgrid-scale (SGS) modelling. Here we treat these scales with effective eddy diffusivities  $\nu$  and  $\kappa$ , which represent momentum and heat transport by unresolved motions in the simulations. For simplicity  $\nu$  and  $\kappa$  are taken as functions of radius alone and in the simulations reported are proportional to  $\bar{\rho}^{-1/2}$ . The Prandtl number  $Pr = \nu/\kappa$  is 0.25 for all simulations.

### 2.2 Our simulations

We are interested here primarily in the interaction between rotation and convection in deep stellar convection zones. In these simulations, we avoid the H and He ionization regions near the stellar surface as well as the stably stratified radiative interior and the tachocline of shear at the base of the convection zone. Thus we are concerned principally with the bulk of the convection zone and our computational domain extends from  $0.72R_{\odot}$  to  $0.96R_{\odot}$ . Solar values are taken for heat flux, mass and radius, and a perfect gas is assumed. The reference or mean state of our thermodynamic variables is derived from a one-dimensional solar structure model (Brun et al. 2002) and is continuously updated with the spherically-symmetric components of the

**Table 1** Simulation parameter space. Evaluated at mid-depth are the Rayleigh number  $R_a$ , the Taylor number  $T_a$ , the rms Reynolds number  $R_e$  and fluctuating Reynolds number  $R'_e$ , the Rossby number  $R_o$  and convective Rossby number  $R_{oc}$ , and the diffusivities  $\nu$  and  $\kappa$  in  $\text{cm}^2/\text{s}$ . The rotation rate of the reference frame  $\Omega_0$  is given in multiples of  $\Omega_{\odot} = 2.6 \times 10^{-6} \text{ rad/s}$  or 414 nHz. Also quoted are kinetic energies relative to the rotating system contained in convection (CKE), differential rotation (DRKE) and meridional circulations (MCKE) in units of  $10^6 \text{ erg cm}^{-3}$  and as a percentage of the total.

case	G1	G5
$\Omega_0$	$1 \Omega_{\odot}$	$5 \Omega_{\odot}$
$R_a$	$3.22 \times 10^4$	$1.29 \times 10^6$
$T_a$	$3.14 \times 10^5$	$6.70 \times 10^7$
$R_e$	84	543
$R'_e$	63	133
$R_o$	0.92	0.28
$R_{oc}$	0.61	0.27
$\nu$	$2.75 \times 10^{12}$	$0.94 \times 10^{12}$
$\kappa$	$11.0 \times 10^{12}$	$3.76 \times 10^{12}$
CKE	3.28 ( 59.0%)	2.11 ( 6.55%)
DRKE	2.26 ( 40.6%)	30.1 ( 93.4%)
MCKE	0.025 ( 0.45%)	0.007 ( 0.020%)

thermodynamic fluctuations as the simulations proceed. We have conducted a number of 3-D hydrodynamic simulations for stars rotating from one to ten times the current solar rate. Here we concentrate on cases at the solar rate (case G1) and at five times the solar rate (G5); the full suite of simulations are discussed at length in Brown et al. (2007). The parameter space explored by these simulations is presented in Table 1. As we probe higher rotation rates, we decrease the eddy diffusivities in the simulation to maintain a comparable level of supercriticality.

## 3 Convection in more rapidly rotating suns

Examples of convective patterns in case G1 and G5 are illustrated in Figure 1. The radial velocity near the top of the domain is presented in Mollweide projection, which displays the entire layer with minimal distortion, with poles at top and bottom and the entire equatorial region displayed in the middle. The convection patterns are complex, time dependent and asymmetric. Owing to the density stratification, the narrow, fast downflow lanes are surrounded by broad, relatively weak upflows. Convection in the equatorial regions is dominated by large cells aligned with the rotation axis whereas at high latitudes the convection is more isotropic and cyclonic. With more rapid rotation, the convection cells decrease in horizontal size and align more strongly with the rotation axis but remain vigorous and turbulent.

A striking finding in our more rapidly rotating systems is the pattern of spatially localized convection evident in Figure 1c. This structure is a region of locally enhanced

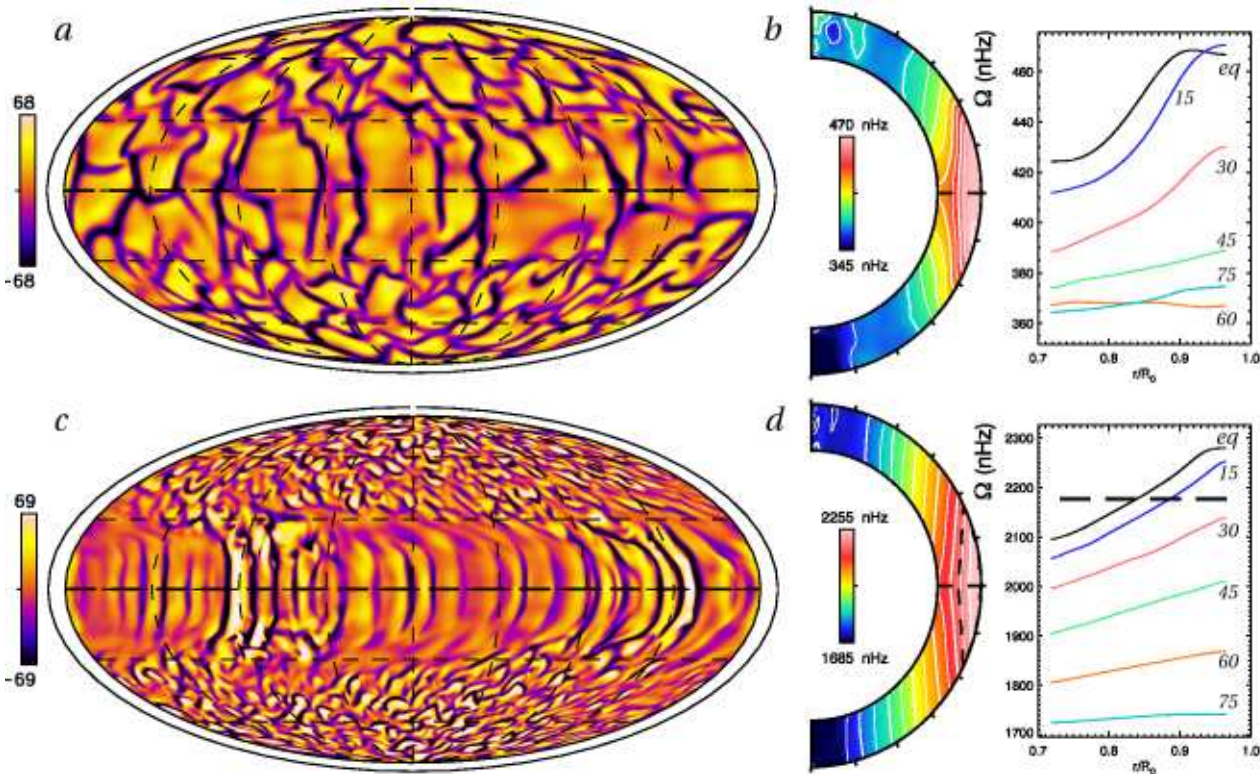


**Fig. 1** Evolution of global-scale convective flows with increasing rotation rate for case G1 (a,b) and case G5 (c,d). Shown in (a, c) are global views, in Mollweide projection, of radial velocity near the stellar surface ( $r = 0.95R_{\odot}$ ). Upflows are light while downflows are dark, with scales indicated in m/s. At high rotation rates a striking pattern of modulated convection emerges at low latitudes, consisting of spatially modulated or patchy convection. Shown in (b, d) are azimuthal averages of angular velocity  $\Omega$  with radius and latitude. These have been further averaged in time over a period of roughly 200 days. Plotted at right are radial cuts of angular velocity at selected latitudes as indicated. The black dashed contour in (d) denotes the constant propagation rate of the nests in such modulated convection.

convection spanning from about  $\pm 30^\circ$  in latitude. Here convective velocities and transport are enhanced, and strong plumes span the depth of the convection zone. This modulated pattern emerges gradually with more rapid rotation and we have found states with either multiple patches of enhanced convection or single isolated patches. At the highest rotation rates, convection in the equatorial regions is present only within the patches, with complex streaming zonal flows in the interpatch regions.

These active nests of convection persist for long periods of time (thousands of days) compared to the typical lifetime of individual convective cells ( $\sim 10 - 40$  days). They propagate in a prograde fashion relative to the stellar rotation rate and with a fixed angular velocity at all depths and latitudes in the equatorial region. The nests of convection are embedded in a strong radial shear, as shown in Figure 1d. Near the surface the mean zonal flow streams through the nests while at depth the zonal flows are slower than the nests. The strong radial shear in the rapidly rotating cases leads to convective structures which are typically double-celled in radius. Near the stellar surface the individual convective cells propagate more rapidly than the nests, with these cells catching up and swimming through the structure. Near the base of the con-

vection zone the nests propagate faster than the individual convective cells.

#### 4 Mean flows and circulations

Differential rotation in our simulations is primarily established by Reynolds stresses from the convection. Convective enthalpy transport in latitude establishes a strong latitudinal temperature contrast in the more rapidly rotating stars, which are largely in thermal wind balance with their differential rotation. The profile of angular velocity realized in case G1 (Fig. 1b) is similar to the solar internal rotation profile, with a fast equator and a monotonic decrease in angular velocity towards the poles. The angular velocity profile realized in this simulation is significantly more columnar than the helioseismically deduced solar internal rotation profile, which is nearly constant on radial lines. Recent simulations (Miesch et al. 2006) reveal that a more solar-like rotation profile can be achieved by including a latitude dependent thermal forcing that is consistent with a tachocline in thermal wind balance. As the nature of tachoclines and the magnitude of this thermal forcing is unclear in other stars, we have chosen here to neglect this latitude dependent thermal

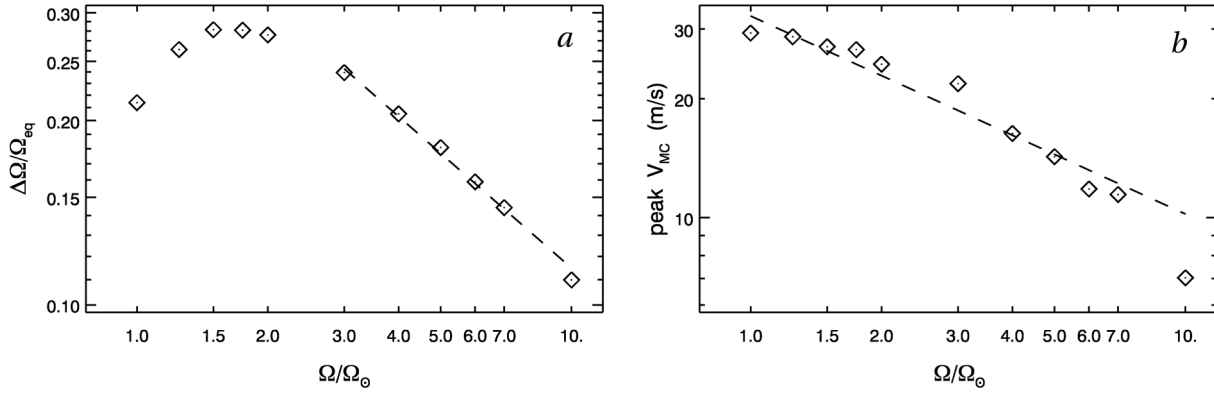


**Fig. 2** Evolution of circulations with faster rotation: (a) angular velocity contrast  $\Delta\Omega/\Omega_{\text{eq}}$  plotted against bulk rotation rate  $\Omega/\Omega_{\odot}$  of the simulations in logarithmic scaling. A power law with exponent  $n = -0.6$  is overplotted. (b) Peak meridional circulations at the top of the simulation ( $r = 0.96R_{\odot}$ ), showing a steep decline with more rapid rotation as the circulations break into multiple cells aligned with the rotation axis. Here a power law with exponent  $n = -0.5$  overlies the data.

forcing and thus our bottom thermal boundary condition is one of constant flux. All of our rapidly rotating stars build angular velocity profiles with fast equators and slow poles. This strong differential rotation is realized even in the most rapidly rotating cases, which exhibit more extreme degrees of convective modulation.

The kinetic energy contained in the differential rotation (DRKE) grows with rotation rate (Table 1). This is accompanied by a growth in the total latitudinal angular velocity contrast  $\Delta\Omega = \Omega_{\text{eq}} - \Omega_{60^\circ}$ . This contrast grows more slowly than linearly with increasing rotation rate, and thus the relative contrast  $\Delta\Omega/\Omega$  decreases in the rapidly rotating simulations (Fig. 2a). Our simulations of rapidly rotating suns appear to roughly follow a power law scaling at the highest rotation rates. However, the actual curve and scaling depends on the parameter space chosen for the simulations, and thus on the level of turbulence achieved, as discussed in detail in Brown et al. (2007).

The energy contained in meridional circulations (MCKE) declines in both magnitude and percentage with more rapid rotation. The decrease in MCKE is accompanied by a decrease in the magnitude of meridional velocities at the surface, as shown in Figure 2b, where we plot the magnitude of the peak time-averaged meridional velocity at the surface. This decrease in circulation strength is accompanied by a change in the topology of the circulations. In case G1, the meridional circulations are largely single-celled in radius and latitude in each hemisphere. In the more rapidly rotating stars, as in case G5, these cells break into multiple weak cells in both radius and latitude, and near the equator these cells align with the rotation axis.

## 5 Conclusions

The complex coupling between rotation and convection drives a strong differential rotation in these more rapidly rotating stars. The meridional circulations in contrast are much weaker, decreasing in both magnitude and relative contribution with more rapid rotation. As such, more rapidly rotating stars may have dynamos which differ substantially from the solar dynamo, where meridional circulations are thought to play an important role. These mean circulations are achieved despite the presence of strong spatial modulation in the convection of the equatorial regions. If these active nests of convection persist in stellar convection zones in the presence of magnetism, they may lead to features at the surface which propagate at rates distinct from that of the surface convection or the zonal flows of differential rotation. Such strong and persistent modulation in convective structures may have important observational consequences.

*Acknowledgements.* This research was supported by NASA through Heliophysics Theory Program grant NNG05G124G and the NASA GSRP program by award number NNG05GN08H. The simulations were carried out with NSF PACI support of PSC and SDSC.

## References

- Brown, B. P., Browning, M. K., Brun, A. S., Miesch, M. S., & Toomre, J.: 2007, ApJ submitted
- Brun, A. S., Antia, H. M., Chitre, S. M., & Zahn, J.-P.: 2002, A&A391, 725
- Brun, A. S., Miesch, M. S., & Toomre, J.: 2004, ApJ 614, 1073
- Charbonneau, P.: 2005, Living Reviews in Solar Physics 2, 2
- Clune, T. L., Elliott, J. R., Glatzmaier, G. A., Miesch, M. S., & Toomre, J.: 1999, Parallel Computing 25, 361
- Donahue, R. A., Saar, S. H., & Baliunas, S. L.: 1996, ApJ 466, 384
- Donati, J.-F., Cameron, A. C., Semel, M., et al.: 2003, MNRAS 345, 1145
- Miesch, M. S., Brun, A. S., & Toomre, J.: 2006, ApJ 641, 618

- Ossendrijver, M.: 2003, *A&A Rev.*11, 287  
Reiners, A. & Schmitt, J. H. M. M.: 2003, *A&A*398, 647  
Thompson, M. J., Christensen-Dalsgaard, J., Miesch, M. S., &  
Toomre, J.: 2003, *ARA&A* 41, 599  
Walker, G. A. H., Croll, B., Kuschnig, R., et al.: 2007, *ApJ* 659,  
1611